

Master Thesis



Czech
Technical
University
in Prague

F3

Faculty of Electrical Engineering
Department of Microelectronics

FastIC+ readout system

Bc. Vojtěch Vosáhlo

Supervisor: Ing. Vít Záhlava, CSc.

Field of study: Electronics

May 2025

Acknowledgements

Declaration

I declare that this work is all my own work and I have cited all sources I have used in the bibliography.

Prague, 25. May 2025

Prohlašuji, že jsem předloženou práci vypracoval samostatně, a že jsem uvedl veškerou použitou literaturu.

V Praze, května 25, 2025

Abstract

This thesis focuses on the design of an electronic system intended for data readout from FastIC+ integrated circuits developed within CERN for precise fast timing applications. The thesis outlines the properties of the mentioned ASICs, their purpose, and describes communication with the chips. Subsequently, it provides a detailed description of the electronics design, firmware development, and final testing of the device. Furthermore, it describes the development of control software for measurements with the device and data interpretation. Finally, it verifies the functionality of the device in a practical experiment.

Keywords: FastIC+, Readout system, Fast Timing, CERN, PCB

Supervisor: Ing. Vít Záhlava, CSc.

Abstrakt

Tato práce se zabývá návrhem elektronického systému určeného k vyčítání dat z integrovaných obvodů FastIC+ vyvíjených v rámci CERN pro aplikace precizního rychlého časování. Práce nastiňuje vlastnosti zmíněných ASIC, jejich účel a popisuje komunikaci s čipy. Následně detailně popisuje návrh elektroniky, firmware zařízení a jejich testování. Dále popisuje návrh ovládacího software pro měření se zařízením a interpretaci dat. V neposlední řadě pak ověřuje funkcionality zařízení na praktickém experimentu.

Klíčová slova: FastIC+, Vyčítací systém, Rychlé časování, CERN, DPS

Překlad názvu: Vyčítací systém pro FastIC+

Contents

1 Introduction	1
2 FastIC+	3
2.1 Detection	3
2.1.1 Time path	4
2.1.2 Energy path.....	4
2.1.3 Trigger path.....	4
2.2 Digitizing	4
3 Aurora protocol	5
3.1 Encoding	5
3.1.1 Data block	5
3.1.2 Separator-7 block	6
3.1.3 Separator block	7
3.1.4 User K-block	7
3.1.5 Idle block	8
3.2 Scrambling.....	8
4 FastIC+ packet structure	9
4.1 Data Packet	9
4.2 Statistics packet	10
4.3 Counter Extension + Event Counter packet	12
5 Device Concept	13
6 Readout Board	15
6.1 Microcontroller	15
6.1.1 Receiving the Aurora stream	16
6.1.2 Omitting clock recovery with the FastIC+	16
6.2 FastIC+	17
6.2.1 I2C communication	18
6.2.2 Calibration pulse generator..	18
6.2.3 Voltage monitoring	18
6.2.4 High speed outputs	19
6.2.5 Trigger input and output ...	20
6.3 USB	20
6.3.1 Clock generation	23
6.3.2 High Voltage	24
6.3.3 Power	26
6.4 Connector	27
7 User board	29
7.1 Sensors	29
7.2 EEPROM	29
8 PCB design	31
8.1 High speed signals	32
8.2 Microcontroller fanout.....	33
8.3 Power integrity	33
8.4 Design files	34
8.5 Manufacturing	35
9 Enclosure Design	37
10 Firmware	39
10.1 USB	39
10.1.1 CDC interface	39
10.1.2 Vendor control.....	39
10.1.3 Vendor interfaces	40
10.2 Clock generation.....	40
10.3 HV power supply	41
10.3.1 PID controller	41
10.4 FastIC+	41
10.4.1 Aurora stream	42
10.4.2 Pulse injection.....	42
10.5 User board	43
11 Software	45
11.1 Device communication.....	45
11.2 Stream processing	45
11.3 Example scripts	45
12 Function verification	47
12.1 Measurements	47
12.1.1 Power supplies.....	47
12.1.2 High Voltage power supply .	48
12.1.3 Pulse injection	49
12.2 Injection pulse test	50
12.2.1 SiPM SPTR measurement .	51
13 Conclusion	53
Bibliography	55
List of abbreviations	57

Figures

2.1 Top-level architecture block diagram	3
3.1 Data block structure	6
3.2 Separator-7 block structure	6
3.3 Separator block structure	7
3.4 User K-Block structure	7
3.5 Idle block structure	8
4.1 FastIC+ data packet structure ..	9
4.2 FastIC+ statistics packet structure	10
4.3 FastIC+ counter extension and event counter packet structure....	12
6.1 Alignment of the sampling clock and data stream	17
6.2 Schematic of the FastIC+ power	17
6.3 Schematic of the FastIC+ logic .	18
6.4 Schematic of the voltage monitoring amplifier	19
6.5 Voltage definition for SLVS transmitter	19
6.6 Schematic of the FastIC+ trigger circuitry	20
6.7 Schematic of the USB connector with ESD protection	21
6.8 Schematic of the USB	22
6.9 Schematic of the UCPD controller	22
6.10 Schematic of the clock generator	23
6.11 Divider for the LVDS to SLVS conversion	24
6.12 High voltage power supply schematic	25
6.13 Sensing of the high voltage and current	26
6.14 Step down regulator schematic	27
6.15 FastIC+ power domain sequencing	27
8.1 High speed signal lines	32
8.2 Microcontroller fanout.....	33
8.3 Top metal layer	34
8.4 Bottom metal layer	34
8.5 Readout PCB	35
8.6 User board PCB	35
8.7 Manufactured readout PCB	36
8.8 Manufactured user board PCB .	36
9.1 Metal insert placement	37
9.2 3D Preview of the Readout PCB Enclosure	38
9.3 Top, Bottom, Front, and Rear Views of the Enclosure	38
10.1 Setup packet structure	40
10.2 EEPROM configuration header structure	43
12.1 Output ripple of the DC/DC converter	48
12.2 Output ripple of the high-voltage power supply.....	48
12.3 Trensient response of the high-voltage power supply	49
12.4 Injected pulse	50

Tables

8.1 PCB stackup	31
-----------------------	----



Chapter 1

Introduction

The development of devices for particle detectors at CERN has often found applications beyond high-energy physics, particularly in the medical field. One such example is the FastIC chip, which was designed for fast timing applications but has been also utilized in positron emission tomography (*PET*) to improve imaging precision. Building on the success of the FastIC chip, a new version, FastIC+, has been developed. This updated version integrates a picosecond Time-to-Digital Converter (*TDC*) for enhanced time measurement capabilities and higher integration. To facilitate the evaluation of the FastIC+ chip's performance, a evaluation board had to be designed to provide a compact and accessible platform for researchers and engineers to test and analyze the chip's capabilities in various applications.

This work describes the design of the evaluation board, referred to as the readout system, developed at CERN. First, the FastIC+ is detailed along with its communication protocol. Subsequently, the hardware concept is proposed, and its key components are described in detail. The hardware design process is presented, and both firmware and host software are developed to enable easy control of the device. Finally, functional tests are conducted to evaluate the device, and an experiment at CERN is performed to verify the functionality of the readout system in a real-world application.

Chapter 2

FastIC+

The FastIC+ is a configurable ASIC for fast timing applications, featuring an 8-channel front-end for photodetectors such as *SiPM*, *PMT*, or *MCP*, capable of precisely measuring the Time-of-Arrival (*ToA*) and Time-over-Threshold (*ToT*) of photons hitting the detectors. This feature set finds its use in applications that require precise photon timestamping, such as Time-of-Flight Positron Emission Tomography, high-energy physics, mass spectrometry, or LIDAR applications. The ASIC is developed in the 65 nm technology by the Institut de Ciències del Cosmos of the University of Barcelona in close collaboration with CERN.

The ASIC can mostly be used without any additional circuitry. Only power and a 40 MHz low-jitter reference clock need to be provided for correct operation. The chip is configured over an *I²C* interface.

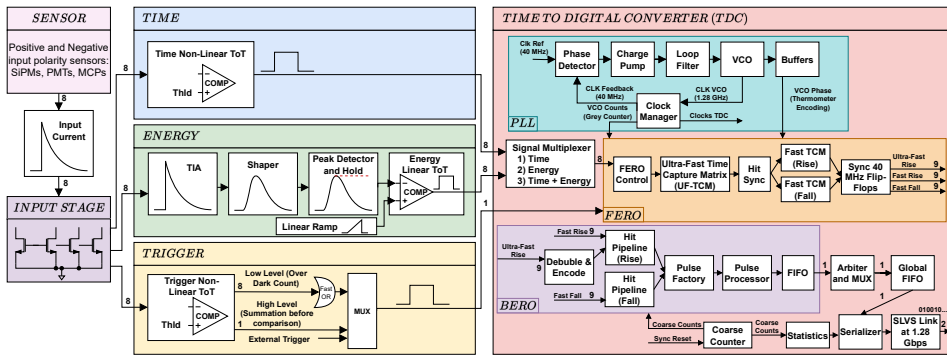


Figure 2.1: Top-level architecture block diagram

2.1 Detection

Each channel of the ASIC consists of a low-impedance input stage, working with both positive and negative polarity sensors with a dynamic range of 5 μ A to 20 mA and stability across sensor capacitances from 10 pF to 1 nF. This stage generates three differently scaled replicas of the input current pulse and forwards them to the three signal paths: time, energy, and trigger.

■ 2.1.1 Time path

The time path acts as a simple discriminator that compares the pulse to a programmable threshold, which can be set down to a single photoelectron level. The leading edge of the comparator output pulse provides the *ToA* timestamp. The logical OR of all time channels can be output via the **TIME** output.

■ 2.1.2 Energy path

The energy path extracts the pulse peak to estimate the energy deposited in the sensor. The chain consists of a transimpedance amplifier, shaper, peak detector with hold, and a comparator that compares the peak detector level with a linear ramp. The length of the output pulse then directly encodes the energy of the pulse. The input can also be compared to a constant threshold to provide a non-linear *ToT* instead.

■ 2.1.3 Trigger path

The final path, the trigger, generates either a low-level trigger per channel or a cluster trigger. The low-level trigger is a logical OR of all the trigger comparators for all channels, whereas the cluster trigger results from an analog summation of the input pulses passed through a single comparator. This trigger can be used internally to trigger the conversion *FSM* or output on a pin. An external trigger can also be injected through a pin.

■ 2.2 Digitizing

The time, energy, and trigger pulses from each channel are passed to a Front-End Readout block (*FERO*), which interpolates the input pulse and generates a digital representation of the rising edge (with a 25 ps time bin) and the falling edge (with a 390 ps time bin).

After capturing the edges, the timing information is sent to the Back-End Readout Block (*BERO*), which processes the data. It corrects signal errors, validates and filters triggers, and encodes the timing information into a suitable binary format. Finally, it stores the encoded packet in the channel's *FIFO* buffer. An arbiter with a multiplexer (*MUX*) then manages requests from all the channel *FIFOs* and stores the packets in a global *FIFO*.

In the final step, an *Aurora* serializer converts the packets from the *FIFO* into an *Aurora 64B/66B* serial stream and transmits them over the high-speed *SLVS* output lines. Statistical and counter information is also transmitted if enabled. The stream can be configured to operate at speeds ranging from 80 Mb/s to 1.28 Gb/s, in compliance with the *Aurora* specification.

Chapter 3

Aurora protocol

Aurora 64B/66B is a link-layer, point-to-point protocol that enables high-speed data transfers between two *Aurora* partners. The *Aurora channel*, established between the partners, can comprise one or more simplex or full-duplex lanes. Data frames are transmitted in 66-bit blocks, consisting of a two-bit synchronization preamble and 64 bits of data. The channel is shared for both data and control messages.

Frame notation and bit order adopted from the *Aurora* specification [1] is used in this chapter, the leftmost bit being the first one transmitted to the bus is considered *MSB*. The rightmost one *LSB*.

3.1 Encoding

As mentioned above, the *Aurora* protocol utilizes the commonly used *64B/66B encoding*. This encoding scheme converts 64 bits of data into a 66-bit block by appending a two-bit preamble. The 0b01 preamble signifies that the block contains 8 octets of data and is therefore called a *Data block*. If the preamble is 0b10, the block is recognized as *Control block* with the most significant octet in the block being a *BTF* (Block Type Field). The remaining 7 octets are data. Preambles 0b00 and 0b11 are interpreted as errors. These preambles are than used by the receiver to synchronize to the data stream.

FastIC+ is capable of transmitting the *Data block* and four of the *Control block* types:

- *Separator-7* block indicated by the *BTF* value 0xE1,
- *Separator* block indicated by the *BTF* value 0x1E,
- *User K-Block* with *BTF* value indicating the ID of the block (see 3.1.4),
- *Idle* block indicated by the *BTF* value 0x78.

3.1.1 Data block

A *Data block*, shown in Figure 3.1, consists of eight octets of raw data. Data blocks are transmitted only when eight or more octets of data are available.

3. Aurora protocol

For smaller packets, the *Separator-7* and *Separator* blocks are used.

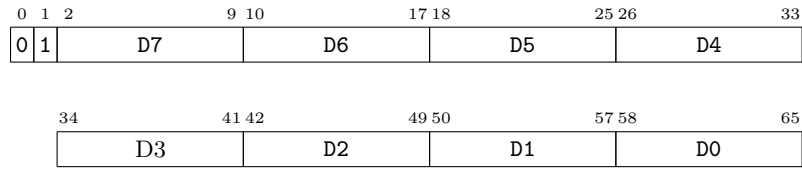


Figure 3.1: Data block structure

■ 3.1.2 Separator-7 block

A *Separator-7 block* is transmitted when only seven octets of data remain to be sent over the interface. The block consists of the *BTF* indicating the *Separator-7* type and seven valid octets of data as shown in Figure 3.2.

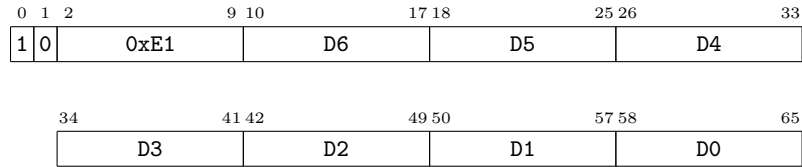


Figure 3.2: Separator-7 block structure

3.1.3 Separator block

A *Separator block* is transmitted when 0-6 octets of data remain to be sent. The block, shown in Figure 3.3, consists of the *BTF* indicating the *Separator* type and a field indicating the number of valid data octets. The order of the valid octets is from *LSB* to *MSB*.

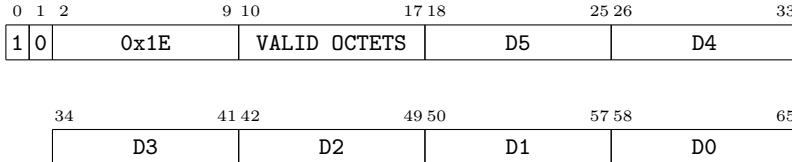


Figure 3.3: Separator block structure

3.1.4 User K-block

User K-Blocks are provided by the Aurora specification to allow the user application to send specific control messages separately from the data. Figure 3.4 shows the *K-Block* comprising the *BTF* and seven data octets. There are nine *K-Blocks* available with IDs 0 to 8, corresponding to *BTFs* 0xD2, 0x99, 0x55, 0xB4, 0xCC, 0x66, 0x33, 0x4B and 0x87, respectively.

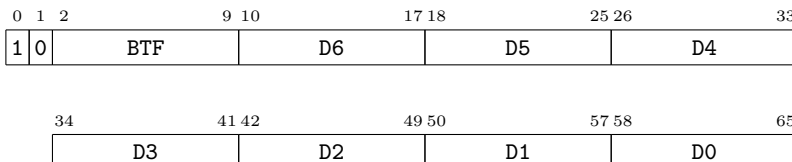


Figure 3.4: User K-Block structure

3.1.5 Idle block

Figure 3.5 shows a structure of an *Idle block*. When no data is available for transmission, *Idle blocks* are transmitted instead to maintain the receivers ability to remain in sync and recover the data clock.

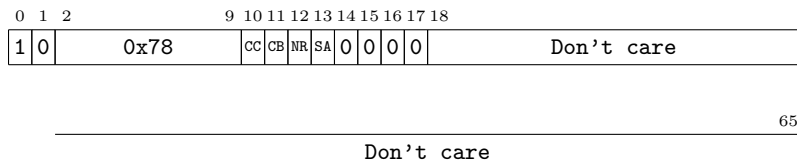


Figure 3.5: Idle block structure

The *Idle block* contains four flag bits determining the type of the block:

- CC bit indicating that the block is *Clock Compensation* idle,
 - CB bit indicating that the block is *Channel Bonding* idle,
 - NR bit indicating that the block is a *Not Ready* idle,
 - SA bit indicating that the receivers obey the *Strict Alignment* rules.

3.2 Scrambling

Whenever either *Data Block* or *Control Block* is transmitted, the eight octets in the block have to be scrambled with the polynomial shown in Equation 3.1. The scrambling serves as a way to randomize the data stream so that a receive can later recover the clock from the bit transitions and synchronize to the stream. Note that the two bit preamble is never scrambled, otherwise, the synchronization could not be acquired.

$$P(x) = 1 + x^{39} + x^{58} \quad (3.1)$$

Chapter 4

FastIC+ packet structure

As mentioned in section 2.2, the ASIC encodes timing and other information into a format suitable for transmission. The structure of these packets is described below.

4.1 Data Packet

Each detection event on each channel of the FastIC+ is represented by one or more 48-bit data packets containing the digitized *ToA* and *ToT* values. The stream of packets is then encoded into *Aurora data blocks*. The structure of the packet is shown in Figure 4.1.

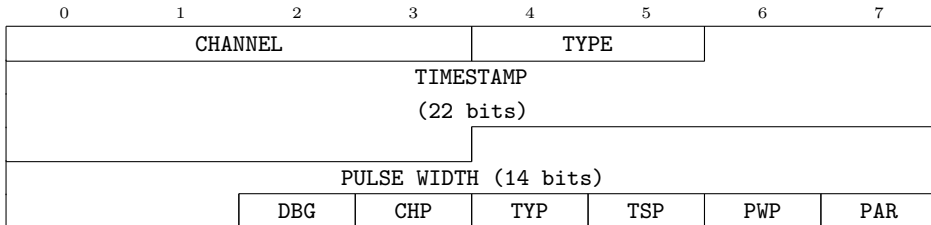


Figure 4.1: FastIC+ data packet structure

The CHANNEL field specifies the channel number where the event was detected, ranging from 0-7 for the inputs or 8 for the trigger channel. The TYPE field indicates the packet type, with the following types being recognized:

- *ToA + non-linear ToT* type represented by the value 0b00,
- *ToA only* type represented by the value 0b01,
- *Linear ToT only* type represented by the value 0b10,
- *ToA + linear ToT* type represented by the value 0b11.

The TIMESTAMP contains the digitized *ToA* value, where each count is 1/1024 of the reference clock period, thus each count is equal to $\frac{1}{40\text{ MHz}} \cdot \frac{1}{1024} \approx 24.4\text{ ps}$. It shall be noted that the timestamp of the packet is relative to the last coarse

counter packet (see 4.3). To reconstruct the absolute timestamp, the coarse counter needs to also be taken into account. The PULSE WIDTH field contains the digitized ToT value with resolution of 1/64 of the reference clock period, thus $\frac{1}{40\text{MHz}} \cdot \frac{1}{64} \approx 390.6\text{ ps}$. DBG is a flag used in debug mode. The rest of the bits are even parity bits, namely:

- CHP parity bit of the CHANNEL field,
- TYP parity bit of the TYPE field,
- TSP parity bit of the TIMESTAMP field,
- PWP parity bit of the PULSE WIDTH field,
- and the overall parity bit PAR computed from all fields.

4.2 Statistics packet

In addition to the data packets, FastIC+ also periodically transmits a statistics packet that contains basic information about the past events. Structure of the packet is shown in Figure 4.2. This packet is sent onto the *Aurora* bus in two *K-Blocks* due to the packet size being bigger than the *K-Block* capacity. The first 56 bits are sent in a block with the *BTF* of 0x99, the rest is sent in a second block with the *BTF* of 0x55.

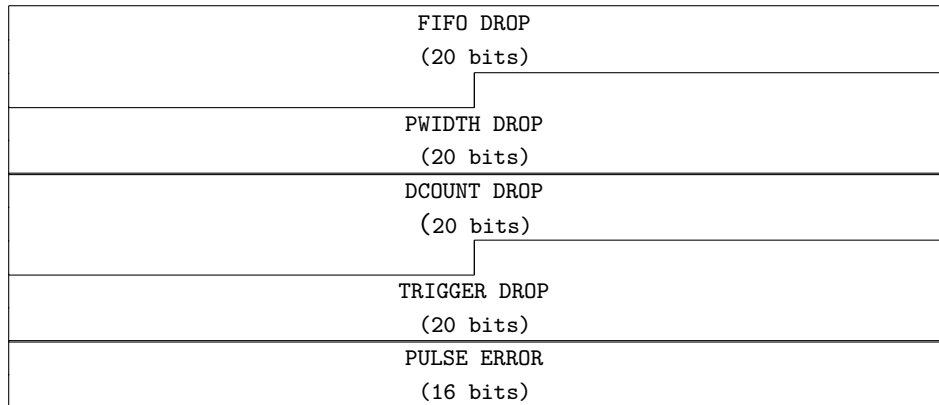


Figure 4.2: FastIC+ statistics packet structure

The packet consists of the following fields:

- FIFO DROP field containing a number of events dropped in the FIFO buffer.
- PWIDHTH DROP field containing a number of events dropped due to the pulse width being outside of the specified range.

- DCOUNT DROP field holding the value of dark counts. This field is valid only if *High-Energy Resolution* mode and *Bandwidth optimization* is enabled.
- TRIGGER DROP field holding the number of packets dropped due to external trigger pulse not being validated.
- PULSE ERROR field being a malformed pulse counter. Malformed pulse is detected when two consecutive edges are read by the *TDC*. This may occur due to the limitation of one leading + falling edge per clock period.

4.3 Counter Extension + Event Counter packet

When no detection events are processed during the *Coarse Counter Extension inactivity period*, the timestamp counter would overflow the **TIMESTAMP** field sent in the data packet. The following packet, specified in Figure 4.3, is transmitted periodically so the receiver can base the absolute data timestamp on the most recent coarse counter value, thus drastically increase the dynamic range of the time detection. The packet is encoded in an *K-Block* with the **BT_F** of 0xD2.

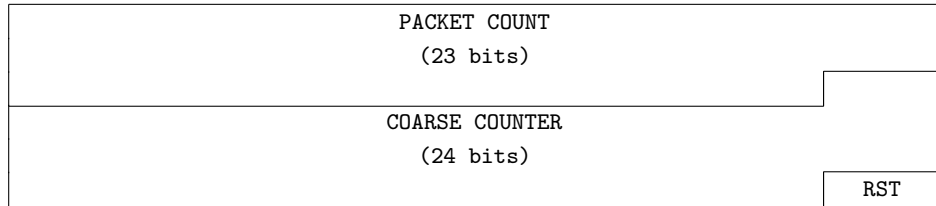


Figure 4.3: FastIC+ counter extension and event counter packet structure

The packets fields are:

- **PACKET COUNT** field, which holds the number of data packets transmitted since the last reset event.
- **COARSE COUNTER** field holding the timestamp from the coarse counter.
- **RST** field indicating, that the coarse counter has been reset during the coarse counter packet period.

The **COARSE COUNTER** field resolution is equal to the period of the reference clock, thus $\frac{1}{40\text{MHz}} = 25\text{ ns}$.

Chapter 5

Device Concept

The ultimate goal was to develop a system utilizing the FastIC+ chips that could be used at CERN to quickly carry out measurements, by companies to simplify prototyping with the FastIC+ chips, or by schools to use them in experiments. This implied the requirements for the system to be:

- versatile to allow for both simple and demanding tasks,
- easy to use for both novices and experts,
- a standalone all-in-one device requiring no external scientific instruments,
- miniature and portable to be taken anywhere,
- financially available for schools and companies.

To allow for versatility, it was decided that two FastIC+ chips would be used, resulting in a total of 16 detection channels. The trigger inputs and outputs were decided to be exposed to the user to allow the synchronization of multiple readout boards. On the other hand, it was decided to read the data from the FastIC+ chips at the lowest possible speed of 80 Mb/s, as it was found sufficient for most applications and would greatly simplify the development.

To make the readout easy to use and standalone, a *USB* interface was proposed to both power the device and transfer the data to a host computer for processing. This, in turn, required the device to be power-efficient and capable of sufficient *USB* bandwidth.

Considering all of the above, it was decided to split the device into two parts:

- the readout board containing all the necessary electronics except the sensors,
- the easily replaceable user board containing mainly the sensors.

Chapter 6

Readout Board

In the typical use case, a system integrating the FastIC+ chip would be based on an *FPGA* with a dedicated *Aurora* receiver or an *FPGA* with a custom *HDL* implementation of the receiver. This approach simplifies the implementation, as *FPGAs* integrate the necessary deserializers and are capable of natively synchronizing to the data stream and reconstructing the data clock. However, the disadvantage is that sufficiently capable *FPGAs* are expensive and power-hungry, which conflicts with the device's requirements. Another issue is that, while implementing an *Aurora* receiver is relatively straightforward, implementing other interfaces like *USB* is complex or requires purchasing expensive *IP cores*. These drawbacks led to the decision to use a microcontroller for the readout system.

When a suitable microcontroller is selected, all the interfaces, such as:

- *ADCs* for monitoring voltages,
- *DACs* for providing voltage feedback,
- *SPI* and *I²C* for communication with other digital devices,
- *USB* for connection to the host,

are implemented in hardware and do not need to be defined in *HDL*. A simple firmware in C/C++ can then be developed to control these interfaces, potentially speeding up and simplifying development while allowing more users to easily customize the device's functionality. The main challenge with this approach is that no microcontroller on the market implements the receivers or deserializers required to recover the clock from the *Aurora* stream and synchronize to it. Therefore, clock recovery must be performed externally, and a suitable alternative peripheral must be chosen to serve as the receiver.

6.1 Microcontroller

The STM32H753XIH6 was chosen as an excellent microcontroller candidate for the system. It is based on an Arm Cortex-M7 core running at up to 480 MHz, which provides the fast computation required for processing the two continuous 80 Mb/s streams. It integrates 2 MB of flash memory and 1 MB of

RAM, which is more than sufficient for buffering the data. From a peripheral perspective, it supports *USB High Speed* with a maximum throughput of 480 Mb/s, which is essential for transferring the large amount of data to the host. It also features multiple *SPI* peripherals supporting input clocks of up to 120 MHz, making them an ideal choice for sampling the *Aurora* stream running at 80 Mb/s, as explained in 6.1.1. The internal data buses of the microcontroller operate at half the core clock speed and support *DMA*, which significantly enhances performance when handling such a large amount of data. In addition to these main features, the chip's implementation of two *ADCs*, one *DAC*, and *I₂C* for digital communication is also beneficial for the readout. The chip is packaged in a compact 14 mm × 14 mm *TFBGA* 240+25 package.

■ 6.1.1 Receiving the Aurora stream

As noted above, the most suitable peripheral for receiving the *Aurora* stream with this microcontroller is the *SPI* peripheral. This peripheral is an industry-standard serial interface, implemented in all modern *MCUs*, designed for receiving a serial stream with a dedicated clock. In simplex slave, receiver-only mode, which suits this use case well, the peripheral uses the *CLK* and *MOSI* pins. The *MOSI* pin is used to input the data stream into the peripheral. The clock, present on the *CLK* pin, is then used to sample the data stream. The sampled data is shifted into a register on a selected clock edge and sent over the internal microcontroller buses for processing. The only challenge with using *SPI* is that the need to recover the clock from the data stream remains.

■ 6.1.2 Omitting clock recovery with the FastIC+

As noted in Section 2, the FastIC+ requires a 40 MHz reference clock to function. The chip features an internal *PLL*, which synchronizes to this clock and distributes it to other peripherals, including the *Aurora* transmitter. Since the *PLL* phase is phase-locked to the input clock, the *Aurora* transmitter, and thus the *Aurora* output stream, is also phase-locked to the input clock, just delayed by the transmitter propagation delay t_{pd} . Measurements have shown that this delay is very stable across a temperature range of 0 °C to 100 °C, with a value of $t_{pd} = (3.48 \pm 0.08)$ ns. If this delay is combined with an additional controlled delay, the digital stream can be aligned such that the data can be sampled with an 80 MHz sampling clock that is in phase with the FastIC+ reference clock.

The delay could be implemented using a variable delay line. However, the t_{pd} of the FastIC+, combined with the typical propagation delay of a common *LVDS-to-CMOS* receiver (typically 5 ns), equals approximately 9 ns. The *Aurora* data stream operates at double data rate, meaning a valid symbol is transferred on both the rising and falling edges of the reference clock. This results in a symbol duration of 12.5 ns. The 9 ns delay, being almost exactly 3/4 of the symbol duration, shifts the data so that both sampling clock edges fall within the data symbol, as shown in Figure 6.1. Consequently, the data

symbol can be sampled on either the rising or falling edge, and the edge can be selected programmatically based on the receiver propagation delay to avoid sampling in a metastable state. Since the FastIC+ outputs an *SLVS* signal and an *MCU* with *CMOS* inputs is used to capture the stream, this receiver must be present anyway. If carefully chosen, it can also serve as the delay line to achieve the correct sampling clock phase, thereby completely eliminating the need to recover the clock from the data stream.

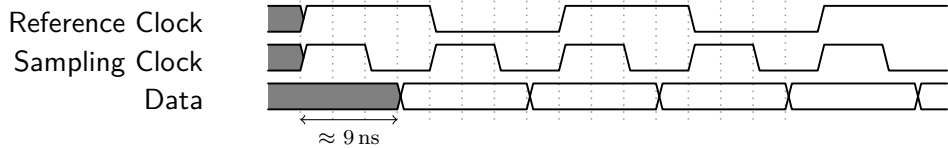


Figure 6.1: Alignment of the sampling clock and data stream

6.2 FastIC+

As mentioned above, the FastIC+ requires almost no additional components aside from a 1.2 V power source and the 40 MHz reference clock. The XVDD (*PLL*) power domain has been isolated from the TVDD (threshold circuitry) by a ferrite bead to reduce noise coupling between the two. However, the *PLL* is only expected to produce noise at startup, while the threshold circuitry is used only after the *PLL* has locked, so any noise coupling between the two domains should have little to no impact. All of the power domains have been thoroughly decoupled, as seen in Figure 6.2.

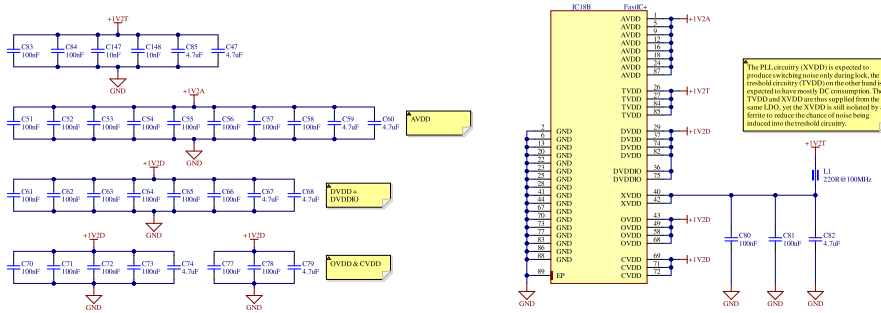


Figure 6.2: Schematic of the FastIC+ power

To increase the stability of the internal bandgap reference, a 10 nF capacitor has been added to the VBG pin according to the datasheet.

Both **nRST** (reset of the FastIC+) and **SRST** (reset of the synchronous counter) have been pulled up to the digital supply so that the microcontroller pins in open drain mode can be used to control these without the need for voltage translation.

6. Readout Board

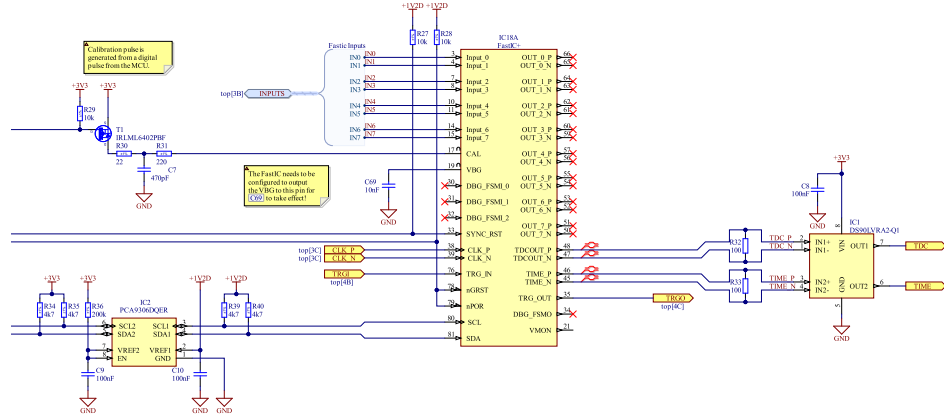


Figure 6.3: Schematic of the FastIC+ logic

6.2.1 I²C communication

As the FastIC+ voltage domains all run at 1.2 V, a voltage shifter had to be implemented for communication with the microcontroller over *I²C*. For this, the PCA9306DQER has been chosen for its miniature *X2SON* package and sufficient 400 kHz speed.

6.2.2 Calibration pulse generator

The FastIC+ features a CAL input pin used for injecting a test pulse into any of the eight input channels. This pin converts the pulse to current with an internal 70Ω resistor. The usual shape of such a pulse should resemble a real sensor output, thus a decaying exponential with an amplitude of a few milliamperes and a length under a microsecond. To create this pulse, a high-side switch has been implemented with series resistance to limit the current and parallel capacitance to recreate the decaying exponential. The transistor gate is driven by a quick digital pulse from the microcontroller, whose length can be adjusted to modify the current pulse width and, to some degree, also the amplitude.

6.2.3 Voltage monitoring

The VMON pin on the ASIC serves for monitoring the internal analog thresholds and *DAC* outputs. Since the microcontroller's internal voltage reference has been selected to run at 1.8 V, a simple non-inverting amplifier with a voltage gain of

$$A_V = \left(1 + \frac{R_{41}}{R_{44}}\right) = \left(1 + \frac{10\text{k}\Omega}{20\text{k}\Omega}\right) = 1.5 \quad (6.1)$$

has been implemented to amplify the 1.2 V output to the microcontroller's full-scale range and improve performance. Because the VMON output is used only for threshold monitoring, thus only DC voltages, a slow RC filter has been used to reduce the noise coupled to the analog signal.

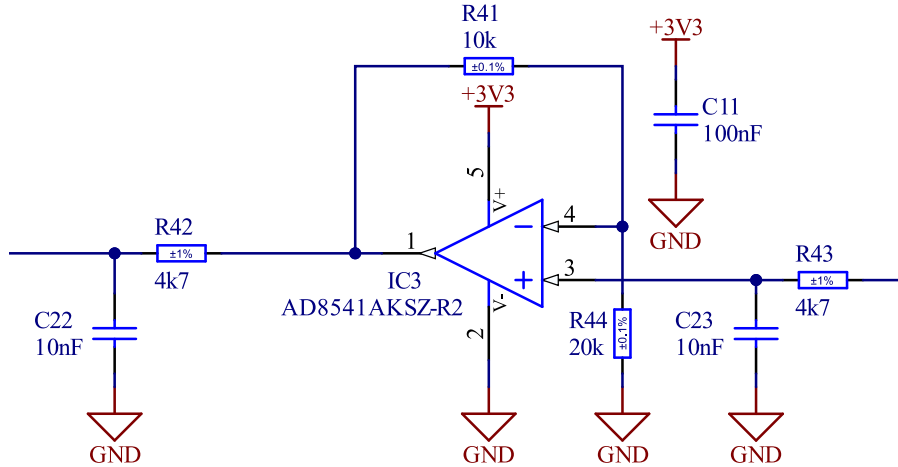


Figure 6.4: Schematic of the voltage monitoring amplifier

6.2.4 High speed outputs

The FastIC+ outputs use the *Scalable Low Voltage Signaling* standard. *SLVS* is an alternative to *LVDS*, utilizing lower voltages. The transmitter common mode voltage V_{CMTX} is 0.6 V, and the differential voltage $|V_{OD}|$ is 0.2 V, as shown in Figure 6.5.

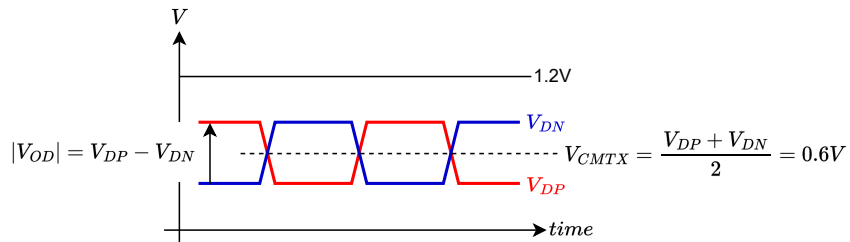


Figure 6.5: Voltage definition for SLVS transmitter

A differential output capable of transmitting a pulse whose beginning timestamps the *ToA* of a photon and whose length resembles the *ToT* is present on the FastIC+ for each channel separately. However, as the readout uses the data digitized by the internal *TDC*, these channels are left unconnected and disabled in the chip to reduce *EMI*.

The *TIME* output can be internally connected to the trigger comparator and used for the trigger threshold calibration routine. That's why it was also interfaced with the microcontroller. When the pin is not used for calibration, it is disabled to reduce any *EMI* generated by the fast edges. The *TDCOUT* is the output of the *Aurora* stream from the transmitter.

Both of the above-mentioned pins are connected to the DS90LVRA2 dual-channel differential line receiver and terminated by a 100Ω resistance, corresponding to the impedance of the differential lines. This receiver, used to convert the *SLVS* output to *CMOS*, has been chosen specifically for its

small size, high enough speed, and typical propagation delay $t_{pd} = 4.4\text{ ns}$ to correctly align the data to the sampling clock. Even though it is intended to convert *LVDS* signals, the threshold voltage levels work well with the *SLVS* standard mentioned above, thus no other special circuitry is needed.

6.2.5 Trigger input and output

The trigger inputs (used for externally triggering the ASIC) and outputs (outputting the signal from the internal comparator) have been exposed to the user on two *SMA* connectors. Termination has been placed on these to mitigate any reflections, and *ESD* protection diodes have been added to protect the chip from electrostatic discharge. It's important to note that the *ESD* diodes add capacitance to the trigger lines, thus degrading (slowing) the trigger edge and introducing a slight delay in the trigger. This either needs to be accounted for when using the readout, or the diodes need to be left unassembled at the expense of worse *ESD* immunity.

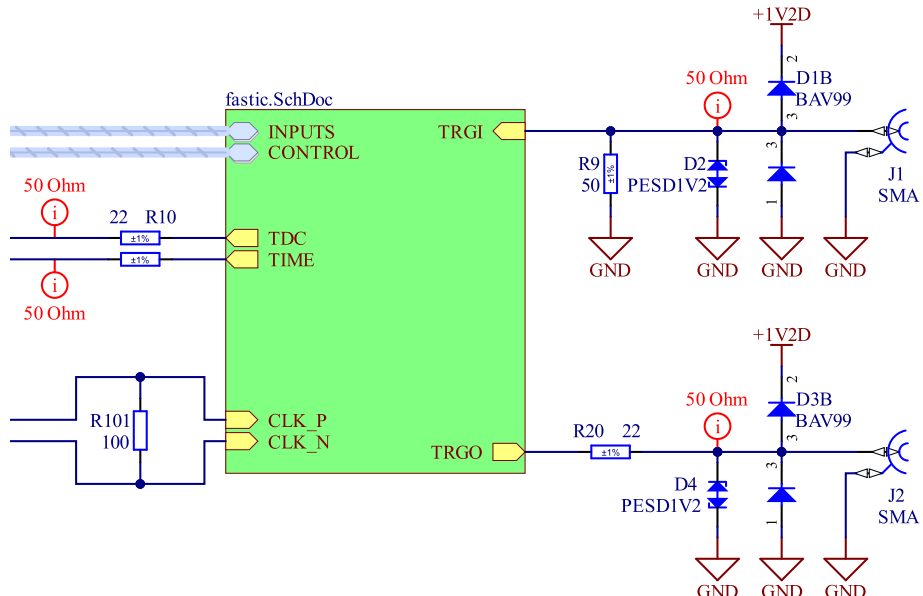


Figure 6.6: Schematic of the FastIC+ trigger circuitry

6.3 USB

To supply power to the device and handle communication with the host computer, a *USB Type-C* connector has been used.

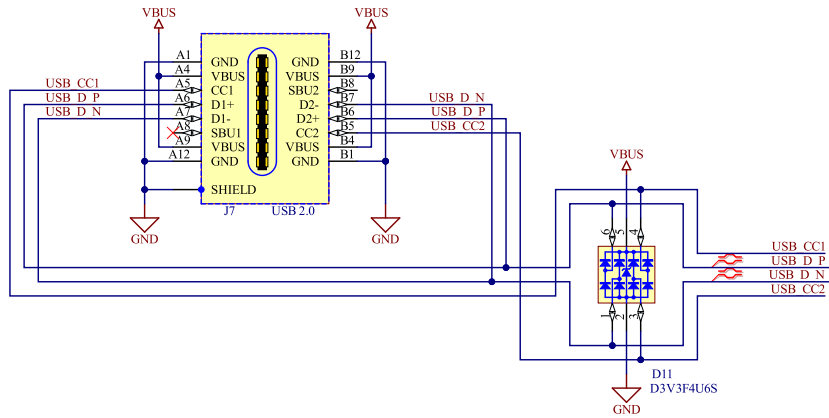


Figure 6.7: Schematic of the USB connector with ESD protection

■ External PHY

Because the combined data rate of the FastIC+ chips of 160 Mb/s exceeds the *USB 1.1* specification, *USB 2.0* (High Speed) was implemented, supporting up to 480 Mb/s throughput. Unfortunately, the microcontroller used does not integrate the *USB 2.0 PHY* directly. Instead, it only integrates the necessary logic and interfaces with an external *PHY* via the *ULPI* interface.

A USB3320 interface was chosen as it is well-supported by the microcontroller and widely used in countless designs. A 48 MHz crystal oscillator has been used as the external reference clock required for the device to operate. Different crystal frequency selections have been made possible with 0Ω resistor jumpers. The *ULPI* connections have been series-terminated to better match the driver output impedance to the controlled impedance of the line.

6. Readout Board

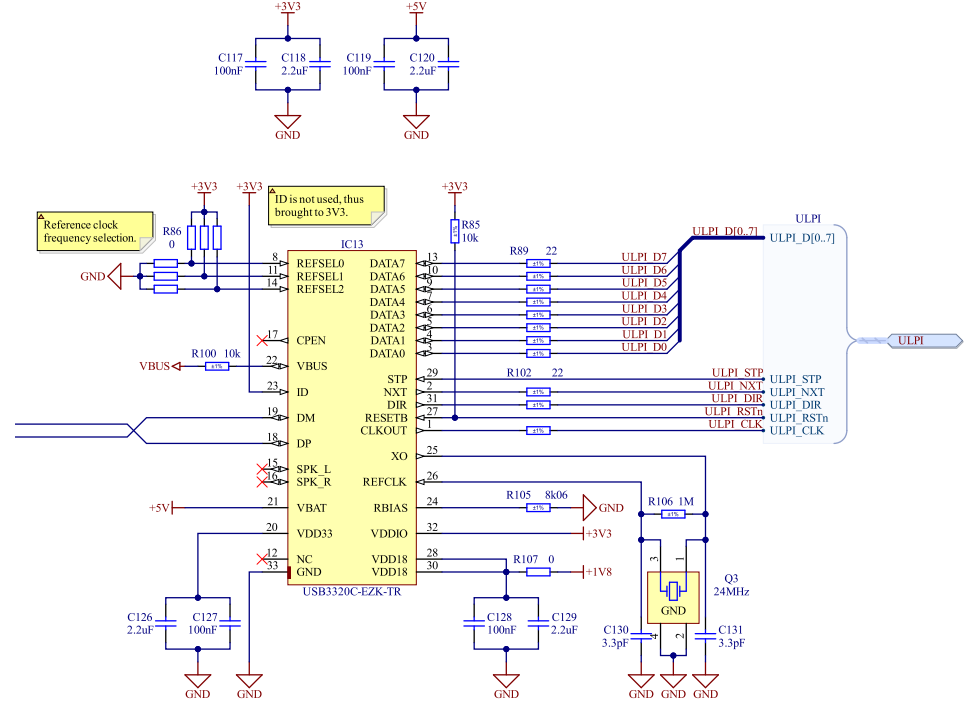


Figure 6.8: Schematic of the USB

■ Power Delivery

A FUSB302 chip was added to allow for power limit negotiation with a UCPD capable power source. The chip handles all the necessary signaling and communicates with the *MCU* via a *I²C* interface. Optional 5.1 kΩ resistors have been added to passively negotiate the highest power limit, if it would be decided to omit the power delivery functionality and not assemble the FUSB302.

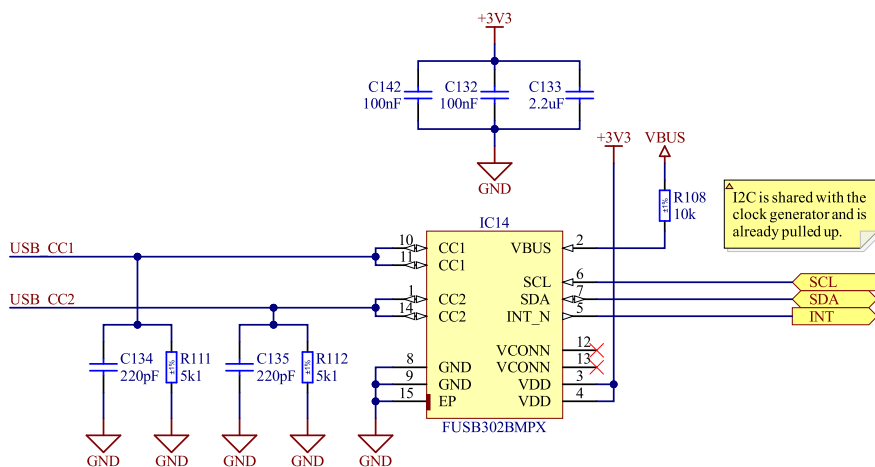


Figure 6.9: Schematic of the UCPD controller

6.3.1 Clock generation

To generate the 40 MHz reference clock for both of the FastIC+ chips and the 80 MHz sampling clock for the *SPI* peripherals, the SI5340 clock synthesizer has been used. It features four outputs with 90 fs *RMS* jitter, supporting both *CMOS* and differential output. Additionally, each output can be powered by an independent power supply, allowing for mixing the 3.3 V *CMOS* signals for the microcontroller and differential signals for the FastIC+. A precise 48 MHz crystal oscillator has been used as the reference clock. The chip features both *I²C* and *SPI* interfaces for configuration. *I²C* was selected for use in this design.

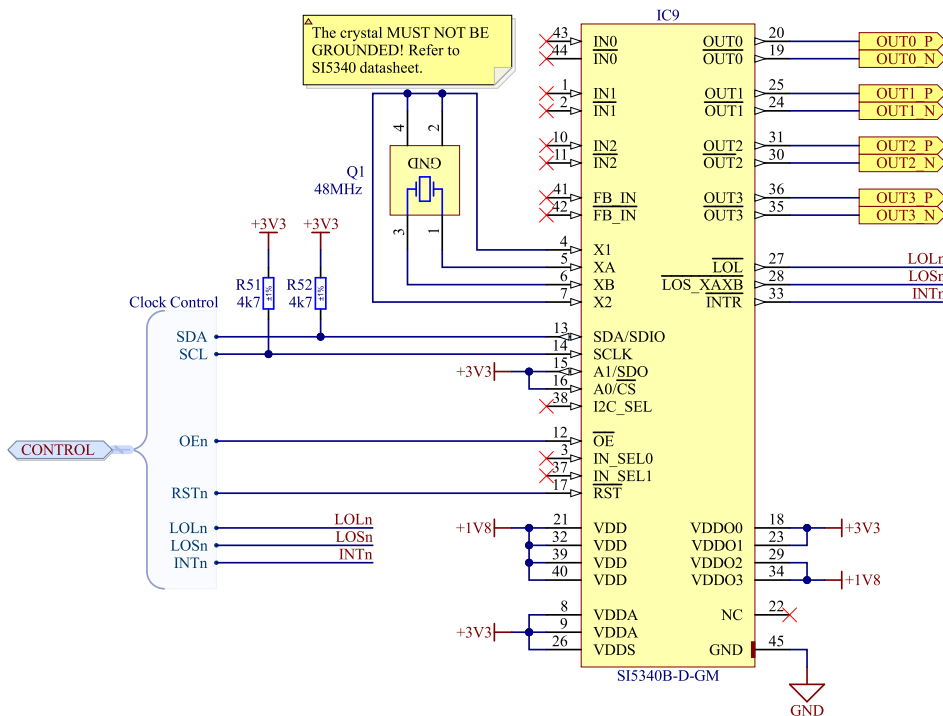


Figure 6.10: Schematic of the clock generator

Since the FastIC+ requires an *SLVS* input, which is not supported by the generator, a signal divider had to be implemented. This circuit, shown in Figure 6.11, was provided in the datasheet to lower the voltage levels while keeping the impedance of the lines well-matched.

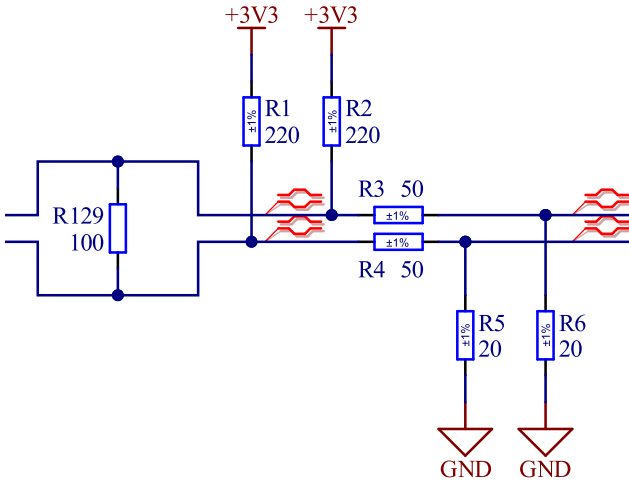


Figure 6.11: Divider for the LVDS to SLVS conversion

6.3.2 High Voltage

All the sensors that the FastIC+ interfaces with, such as *SiPMs*, *PMTs*, or *MCPs*, require high-voltage biasing for their operation. To eliminate the need for an external high-voltage supply, an internal one has been implemented using the LT3571. This DC/DC converter, designed for biasing avalanche photodiodes, is capable of generating up to 75 V output from a low-voltage input. It fully integrates the power switch and regulation along with soft-start and variable switching frequency. This has been set to approximately 1 MHz via R61. A higher switching frequency allowed for the use of smaller inductance, thereby keeping the size of the device compact.

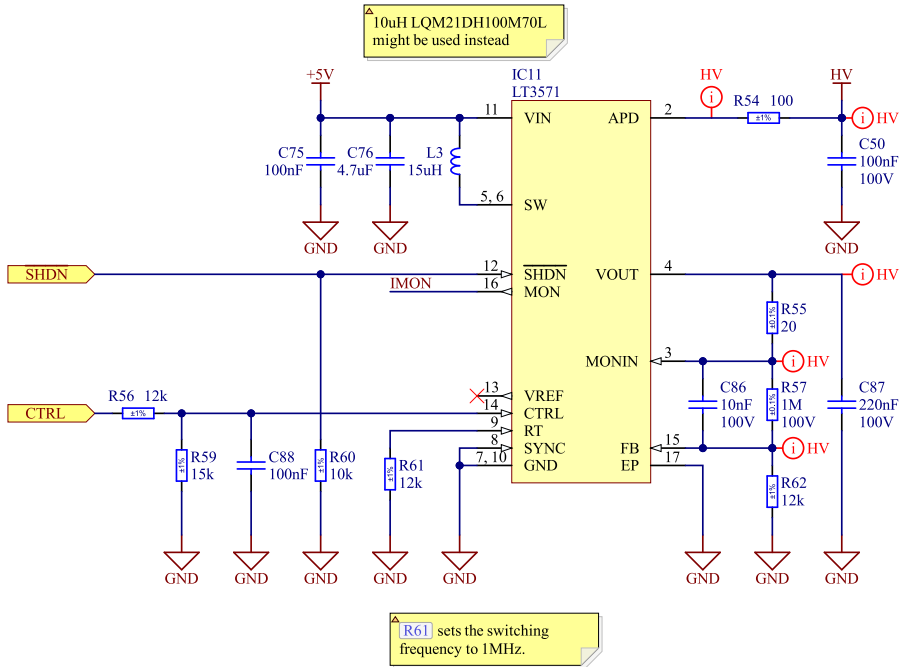


Figure 6.12: High voltage power supply schematic

A CTRL input is available for adjusting the output with a control voltage. This reference is generated by the *MCU DAC* and divided by a voltage divider to a suitable 0 V - 1 V range. The feedback resistor divider was chosen such that the theoretical maximum output voltage, with the CTRL pin held at 1 V, is 84.3 V, as shown in equation 6.2.

$$V_{MONIN} = \left(\frac{R57}{R62} + 1 \right) \cdot V_{CTRL} = \left(\frac{1000 \text{ k}\Omega}{12 \text{ k}\Omega} + 1 \right) \cdot 1 \text{ V} = 84.3 \text{ V} \quad (6.2)$$

The current limit resistor has been chosen to limit the APD pin current to approximately 8 mA based on the equation 6.3 mentioned in the datasheet.

$$R_{SENSE} = \frac{200 \text{ mV}}{1.2 \cdot I_{APD} + 0.3 \text{ mA}} \approx 20 \Omega \quad (6.3)$$

where I_{APD} is the APD pin current limit in milliamperes. To allow for closed-loop control with the microcontroller, the output voltage on the APD pin is monitored via a suitable voltage divider with an operational amplifier buffer. For current monitoring, the LT3571 offers the IMON pin, which sources a current $I_{IMON} = 0.2 \cdot I_{APD}$. This current is then converted to voltage with a $1\text{ k}\Omega$ resistor and buffered with an operational amplifier.

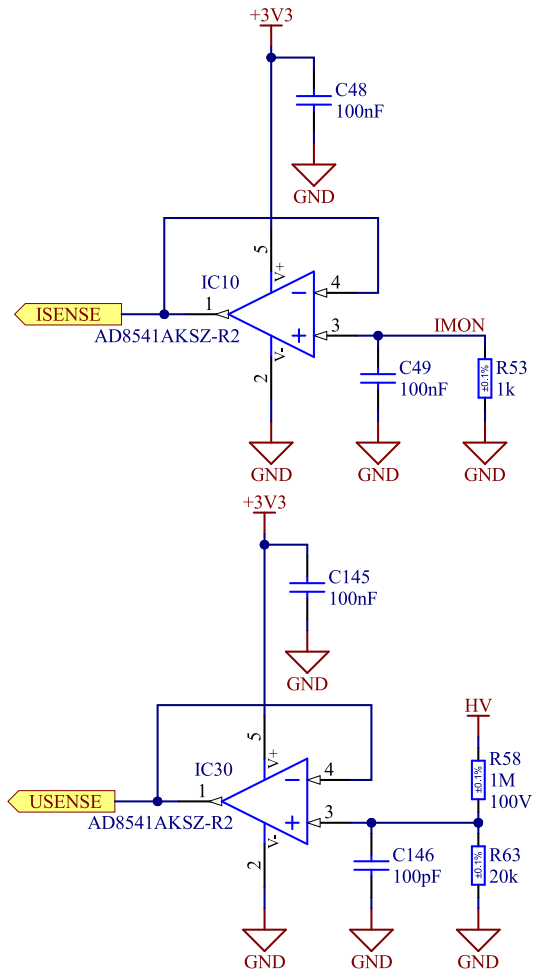


Figure 6.13: Sensing of the high voltage and current

6.3.3 Power

A DC/DC converter has been implemented to efficiently lower the 5 V input voltage to the 3.3 V used by the microcontroller. The 3.3 V for the analog domain has been generated with a low ripple *LDO*. The 1.8 V domain for the *USB* interface has been derived from the 3.3 V using an *LDO* aswell, as efficiency is not required with the low power consumption of 29.4 mA of the 1.8 V domain.

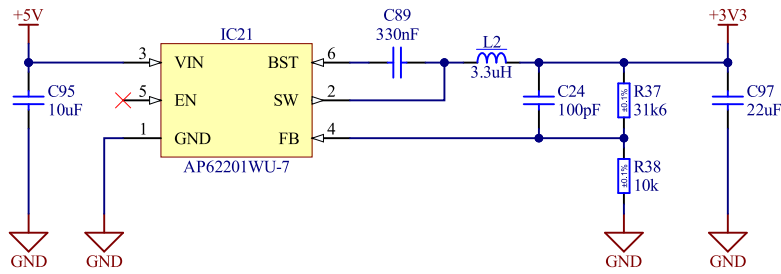


Figure 6.14: Step down regulator schematic

Power sequencing has been implemented for all the three FastIC+ voltage domains. First, the digital domain supply is activated, followed by the supply for the threshold circuitry and *PLL* and lastly, the analog domain is supplied. All of these domains are derived from the 3.3 V using a 1.2 V *LDOs* which are sufficient for the low power consumption (113 mA per chip) and provide a ripple-free supply for the sensitive threshold circuitry.

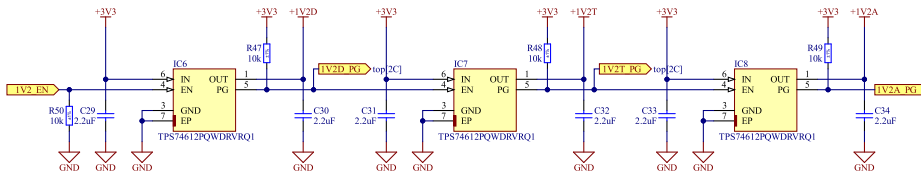


Figure 6.15: FastIC+ power domain sequencing

6.4 Connector

To interface with the user board, the 9 mm high version of the ERM8-020 connector has been used due to its durability (up to 1000 connection cycles), good high-speed performance, and suitable pin count. This connector carries all sixteen input channels alongside the high-voltage biasing supply. The 3.3 V supply is also exposed, and four pins are dedicated to user board identification.

Identification pins

The identification pins serve as an easy way to assign a four-bit short ID to a specific user board. This ID can then be used by the software to load a configuration preset defined for the user board. If the user board designer decides to, the pins *ID0* and *ID1* can be used as *I₂C* communication lines. A compatible *EEPROM* can then be assembled on the user board, making it possible to save the full configuration on the user board itself, as well as additional data such as the name or a unique ID. If the *I₂C* interface is to be used, all of the ID pins need to be pulled up high by a suitable resistor. At least one of the ID pins has to be high at all times. This means that an ID of 0b0000 is not allowed, and in this case, the readout will not recognize a valid user board.

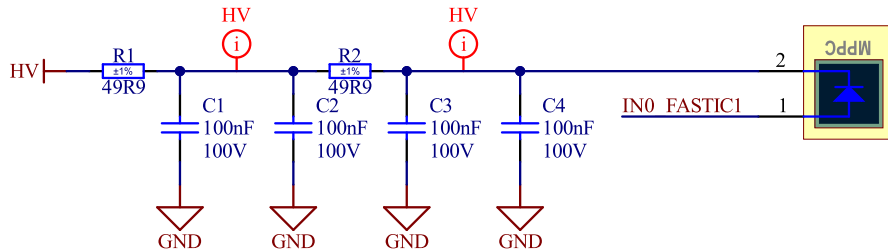
Chapter 7

User board

The user board has been developed as a template for users to easily get started with the readout system. It contains a matrix of 4×4 *SiPM* sensors as well as an *EEPROM* for storing the board configuration. The 9 mm high ERF8-020 connector has been chosen for the user board to match the counterpart present on the readout and allow enough clearance between the assembled readout board and user board.

7.1 Sensors

The footprint for generic THT *SiPMs* has been implemented on the board. Each *SiPM* is biased with the high voltage, and the input is filtered with a dual RC low pass to eliminate the possibility of cross-triggering of the sensors.



7.2 EEPROM

The 24AA04T-I/OT 4 kb *EEPROM* has been used on the user board for the configuration storage. It has been selected for the low price and sufficient capacity.

Chapter 8

PCB design

Special care had to be taken when designing the PCB, keeping in mind the correct design practices for proper power integrity, signal integrity and high speed design.

First a suitable stackup was chosen. In this case, it was decided to proceed with an eight layer stackup as shown in table 8.1.

Table 8.1: PCB stackup

Layer	Name	Thickness
1	L1 - Top copper	0.018 mm
	Dielectric - PR2116	0.120 mm
2	L2 - Ground plane	0.035 mm
	Dielectric - FR4 core	0.200 mm
3	L3 - Power plane	0.035 mm
	Dielectric - PR2116	0.120 mm
	Dielectric - PR2116	0.120 mm
	L4 - Signal layer	0.035 mm
4	Dielectric - FR4 core	0.200 mm
	L5 - Signal layer	0.035 mm
	Dielectric - PR2116	0.120 mm
	Dielectric - PR2116	0.120 mm
6	L6 - Power plane	0.035 mm
	Dielectric - FR4 core	0.200 mm
7	L7 - Ground plane	0.035 mm
	Dielectric - PR2116	0.120 mm
8	L8 - Bottom copper	0.018 mm

The layers 2 and 3, as well as layers 6 and 7, were completely dedicated to ground and power planes. This, in combination with relatively thin dielectric in between, creates inherent capacitive coupling between the planes proportional to the plane area and spacing, which helps the power integrity of the device. Leaving the planes solid also keeps the impedance minimal which reduces the voltage drops. The layers 4 and 5 were also mostly kept as planes, although some connections needed to be routed through these because of the very high board density. While routing in these layers, care was taken not to

cross possible return current paths of the planes with another trace, which could result in a much bigger current loop and an increase in *EMI*. Layers 1 and 8, the top and bottom copper, were used mainly for routing of all the signals. Since both of the layers have a ground plane underneath, both of them were used for routing of the high speed lines with defined impedance.

8.1 High speed signals

To mitigate possible reflections on the high-speed lines carrying high-frequency signals, the characteristic impedance of each line was calculated to match the driver impedance. For differential signals, the differential impedance was optimized to be $100\ \Omega$, except for the USB lines, which require a differential impedance of $90\ \Omega$. For single-ended lines, the target impedance was $50\ \Omega$. The line widths, as well as the spacing for differential pairs, were calculated using Altium Designer's impedance calculator and verified using the PCB manufacturer's impedance calculation tool. These calculations resulted in a width of $W_{USB} = 0.183\text{ mm}$ and spacing of $S_{USB} = 0.2\text{ mm}$ for the USB differential pair; a width of $W_{DIFF} = 0.15\text{ mm}$ and spacing of $S_{DIFF} = 0.2\text{ mm}$ for the remaining differential pairs; and a width of $W_{SE} = 0.182\text{ mm}$ for all single-ended high-speed lines. The spacing from the ground plane on these was kept as large as possible to avoid affecting the impedance. These widths and spacings were followed during PCB routing to ensure the trace impedances remained as close to their respective targets as possible. Where necessary, the line lengths and skews were matched. Routing of the *ULPI* interface and FastIC+ clock lines can be seen in Figure 8.1.

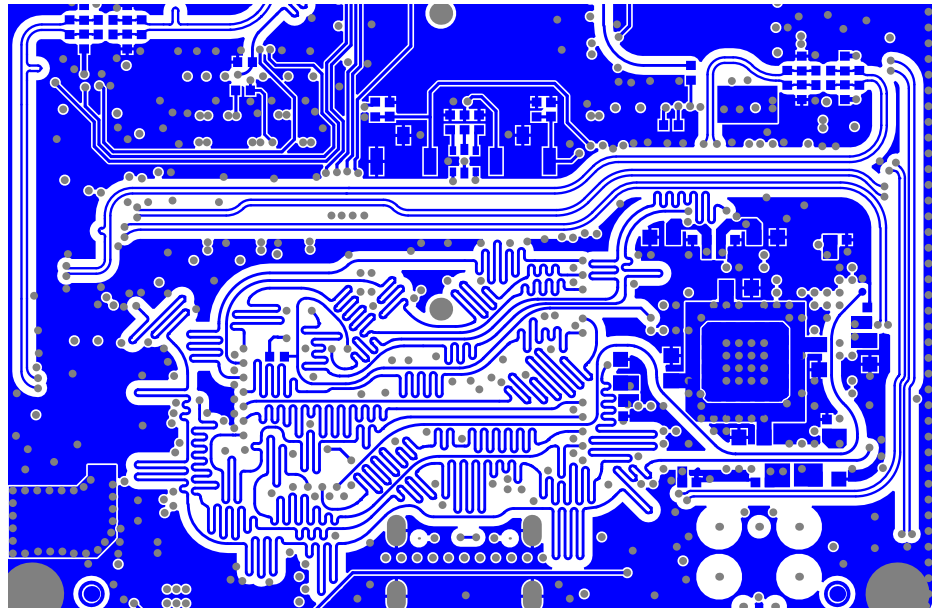


Figure 8.1: High speed signal lines

8.2 Microcontroller fanout

Care was taken to properly fan out the microcontroller pins to avoid any signal integrity issues. First, the pinout was optimized to place the high-speed lines along the perimeter of the package, allowing them to be routed as directly as possible. Decoupling capacitors were then placed on the bottom side of the PCB, as close to the power pins as possible, in order to minimize connection inductance and current loop area. The remaining low-speed connections were routed in the leftover space. Routing under the microcontroller can be seen in Figure 8.2.

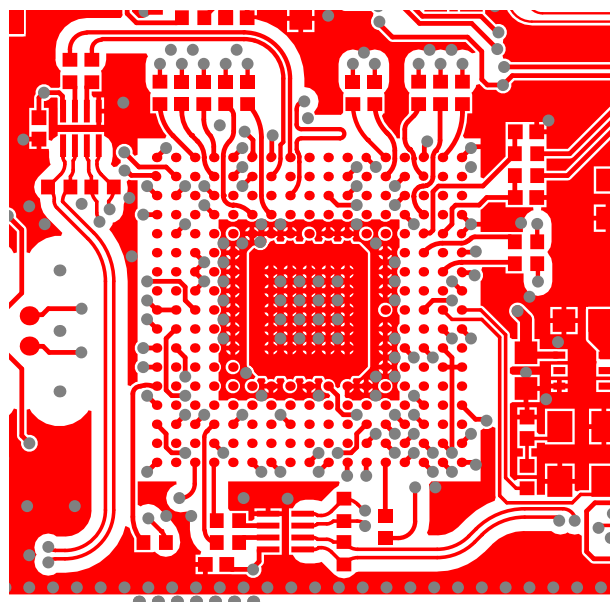


Figure 8.2: Microcontroller fanout

8.3 Power integrity

The power integrity of the device was ensured by using solid power and ground planes, as previously described. Capacitors were placed as close as possible to the power pins of the decoupled integrated circuits and connected to the planes using vias, in order to minimize the inductance of the current loops. The ground planes were stitched together with via array. Additional care was taken to place ground vias near locations where high-speed lines transition between the top and bottom *PCB* layers. Since the current of a high-speed signal in a transmission line is concentrated in close proximity to the signal trace, the corresponding return current flows along the adjacent ground plane. By placing ground vias next to the signal vias, the return path is preserved, minimizing the loop area and reducing emitted *EMI*.

8.4 Design files

Gerber files were generated using Altium Designer and were made available on the *GitHub* repository. The PCB was designed to be as compact as possible, with a size of 50 mm × 50 mm. Top and bottom layers can be seen bellow.

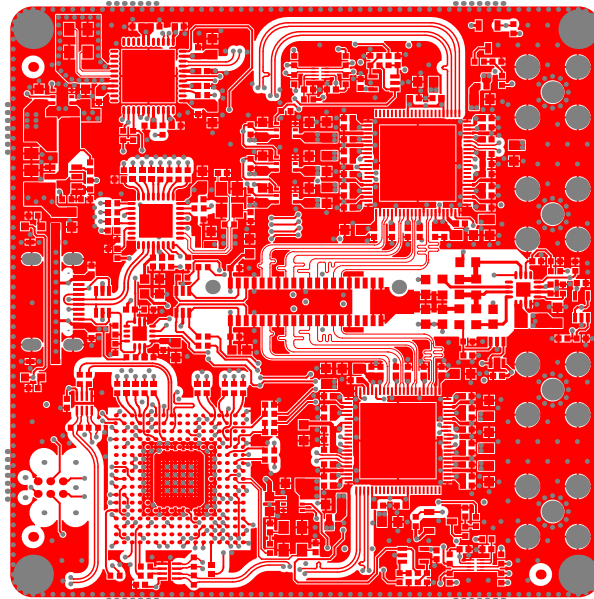


Figure 8.3: Top metal layer

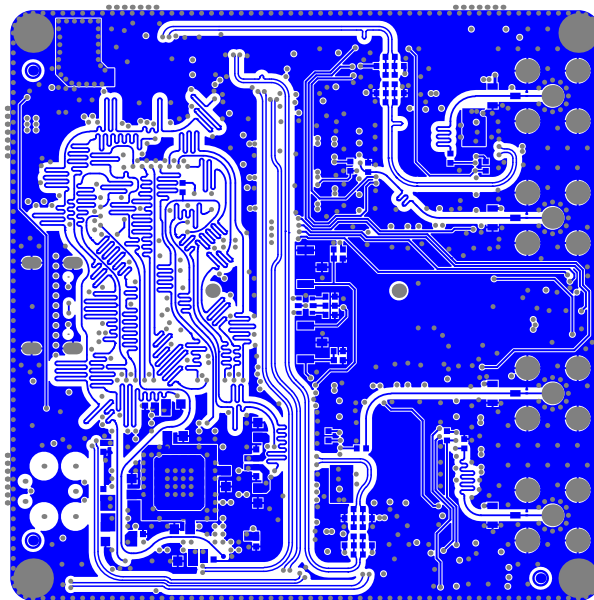


Figure 8.4: Bottom metal layer

8.5 Manufacturing

The two PCBs described above were manufactured and assembled by Eurocircuits. The 3D renders as well as actual photos of the assembled PCBs can be seen in the images below.

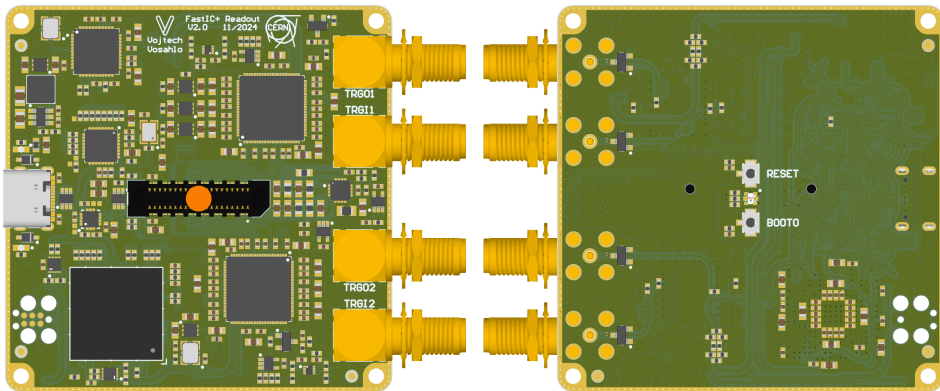


Figure 8.5: Readout PCB

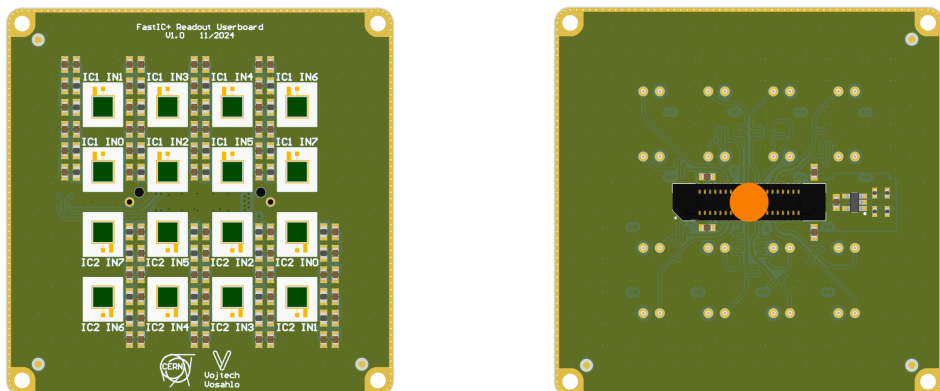


Figure 8.6: User board PCB

8. PCB design

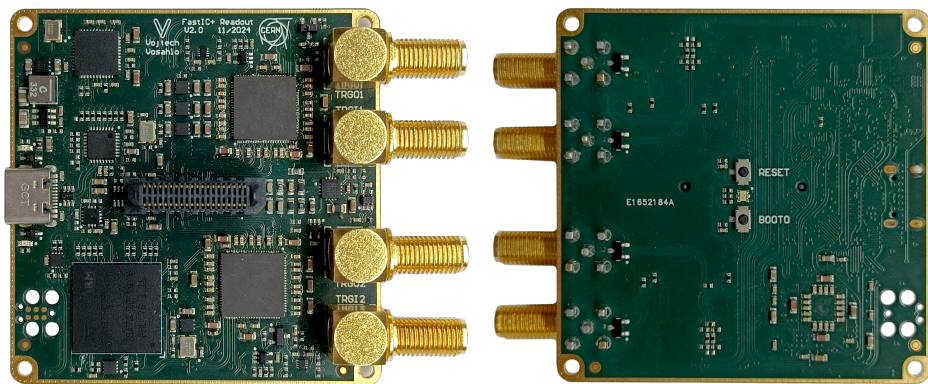


Figure 8.7: Manufactured readout PCB

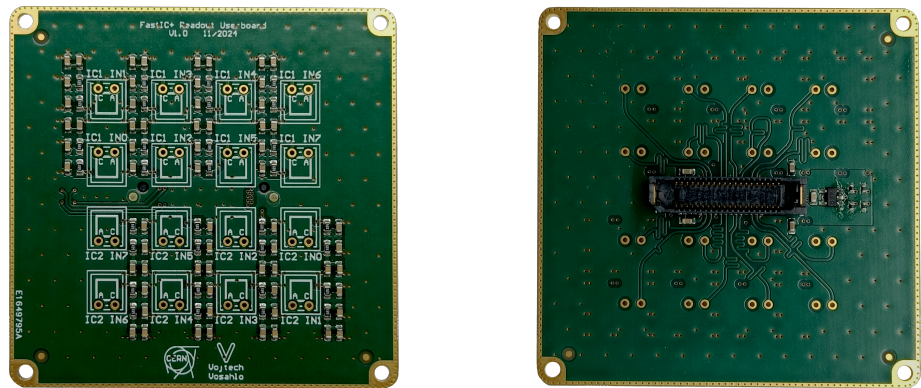


Figure 8.8: Manufactured user board PCB

Chapter 9

Enclosure Design

To complete the device design, a custom enclosure was created to house both the readout PCB and the user board. The enclosure is designed to protect the sensitive electronics while ensuring adequate airflow for thermal management. It consists of three main components:

- **Bottom Shell:** This part includes holes for the reset button, boot button, and LED indicator.
- **Sleeve:** This section features cutouts for all the SMA connectors and the USB port.
- **Top Shell:** This piece fully encloses the readout PCB.

Holes for metal heat inserts are located in the corners. Once the inserts are in place, the three parts are secured together using four M2 screws. The user board can be easily disconnected from the readout PCB. If needed, it can also be fixed in place using M2 screws. The placement of the inserts and screws is depicted in Figure 9.1.

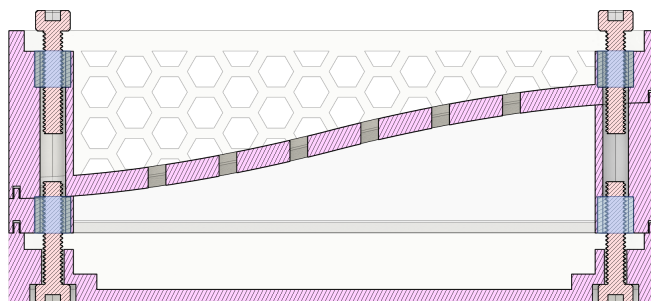


Figure 9.1: Metal insert placement

The enclosure was designed to be 3D printed using a standard *FDM* printer. The top shell and sleeve can either be printed separately and glued together, or they can be printed as a one piece on multi material printer. The design process was carried out in Fusion 360. Renders of the enclosure are shown below.

9. Enclosure Design

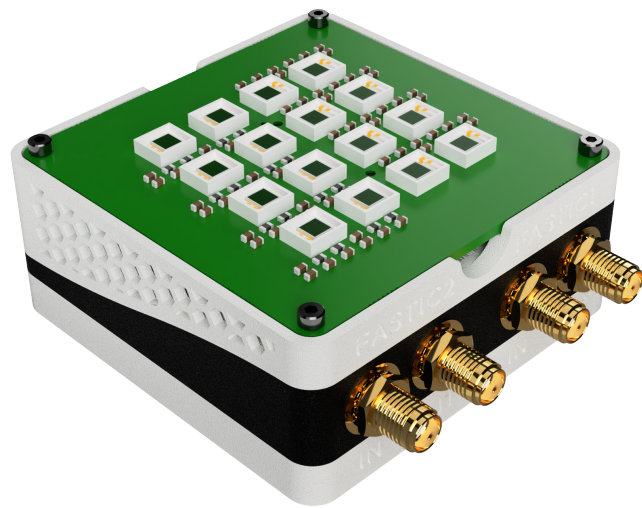


Figure 9.2: 3D Preview of the Readout PCB Enclosure

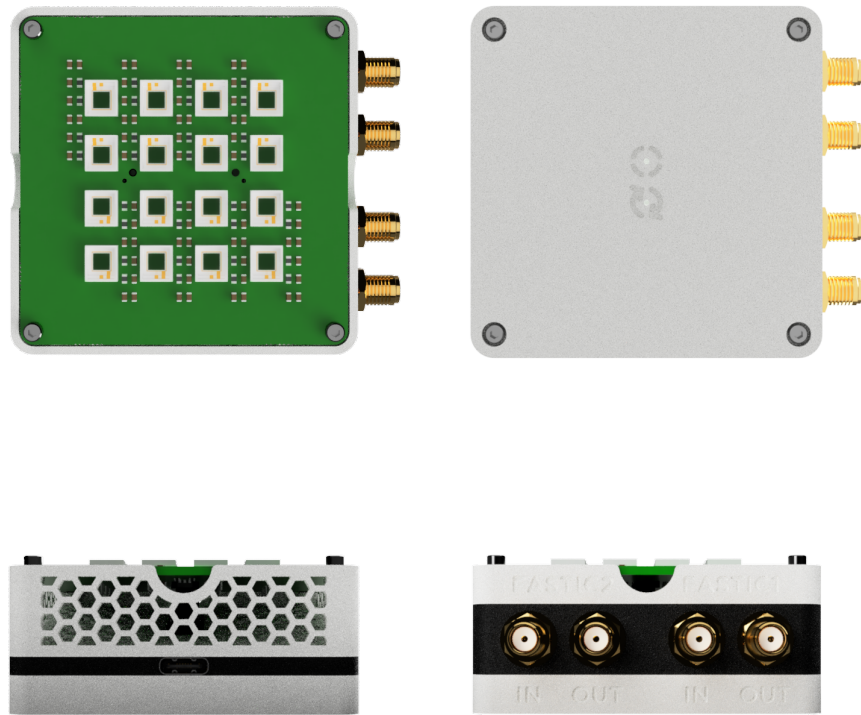


Figure 9.3: Top, Bottom, Front, and Rear Views of the Enclosure

Chapter 10

Firmware

Firmware in the C++ programming language has been developed for the readout, aiming for the best performance and reliable functionality.

10.1 USB

The TinyUSB library has been used for implementing the USB stack on the device. It is an open-source cross-platform USB stack for embedded systems, designed to be memory-safe with no dynamic allocation and thread-safe. It provides support for both Host and Device roles and implements all the common USB classes such as CDC, HID, DFU, Vendor-specific, and others. On the STM32H7 series specifically, it is capable of working with the ULPI PHY in HS mode and making use of the internal DMA to allow for very high throughput and good latency. All of these specifications make it ideal for this application.

Three interfaces have been implemented to allow for the configuration of the device via a human-readable protocol, binary protocol, and readout of the two data streams.

10.1.1 CDC interface

A *Communication Device Class* has been implemented on the first interface (endpoints 0x81, 0x82, and 0x02). This interface emulates a COM port over USB and allows for easy, human-readable interaction with the device. A simple text protocol has been implemented to serve all the required functions of the device. The available commands were documented on the GitHub page of the project.

10.1.2 Vendor control

The USB specification describes a way to communicate with a USB device in a bursty manner by *Control Transfers*. A *Control Transfer* is typically a short random packet, containing up to 64 B of data, which is delivered to the default endpoint with best-effort delivery (no retransmissions). These packets are, for example, used to control the flow of the *CDC* interface but

can be very easily adapted to transfer auxiliary vendor data and thus allow for binary communication with the device.

The same commands as in the *CDC* interface have been implemented using control transfers to allow for easier interactions with the device via software on the host, as the text communication adds unnecessary overhead.

A control transfer is started by an eight-byte-long *Setup Packet*, which contains the following fields:

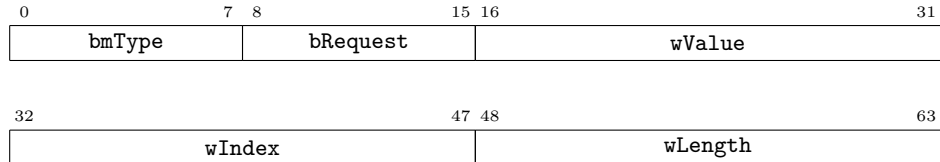


Figure 10.1: Setup packet structure

The **bmType** field indicates:

- the direction of the communication,
- the type, in this case, a Vendor transfer,
- and the recipient, in this case, a Device.

The **bRequest** field indicates the request number. The readout text commands have each been mapped to a unique number, which is used in this field in the binary communication. **wValue** and **wIndex** allow for other parameters to be passed with the request, such as the index of the FastIC+ chip or the address of the selected register. If there is more data to be transferred, the **wLength** field is used to specify the length of an additional data packet sent after the *Setup Packet*.

10.1.3 Vendor interfaces

For transferring the *Aurora* data stream from the FastIC+ chips to the host, two vendor interfaces have been implemented, one for each FastIC+ chip. The sampled bitstream is transferred using *Bulk Transfers* over these two interfaces.

10.2 Clock generation

The configuration for the Si5340 clock synthesizer was generated using the *Clock Builder application* provided by Skyworks. This software generates a register map as a C/C++ array that is later parsed by the software, and the configuration is applied to the synthesizer over *I²C*.

10.3 HV power supply

For controlling the high-voltage power supply, a *DAC* peripheral has been used to provide the control voltage. Two channels of an *ADC* peripheral with 256 times oversampling, resulting in a 1000 Hz sample rate, were then used to acquire feedback for voltage and current monitoring.

10.3.1 PID controller

A closed-loop *PID controller* was implemented using the *ADC* inputs and *DAC*. This controller calculates the *DAC* value to minimize the difference between a required output voltage and feedback from the *ADC*. On every cycle, which takes place after the *ADCs* finish sampling, an error value e is calculated, representing the difference between the setpoint and the measured voltage. The error is then integrated into the variable I , and a derivative of the measured value is calculated, denoted D . In the end, a corrective output setting is calculated to compensate for possible error using the following equation:

$$O = K_P \cdot e + K_I \cdot I + K_D \cdot D \quad (10.1)$$

where O is the output value, and K_P , K_I , and K_D are the proportional, integral, and derivative constants, respectively.

The aforementioned constants can either be determined analytically after modeling the control loop's transfer function, heuristically (for example, by the Ziegler-Nichols method), or manually, which was chosen in this case. First, the proportional constant was set to a value that would bring the output close to the desired value while not causing any oscillations. Then, the integral part was increased to minimize the steady-state error but kept safely below any oscillation threshold. Overshoots and undershoots of the regulator were examined with every change. Finally, the derivative part was added to improve the dynamic response, and the performance was tested. The values of $K_P = 150$, $K_I = 3$, and $K_D = 10$ were found to be suitable for the regulator.

10.4 FastIC+

Both of the FastIC+ chips are mainly controlled over the *I²C* interface. Only a very basic configuration is done by the software, setting the proper clock dividers to be able to receive the *Aurora* stream. Rest of the settings are left for the user to modify, as the registers of the FastIC+ can be accessed directly over the communication interface and most of them need to be tuned for a specific application of the readout.

■ 10.4.1 Aurora stream

When enabled by a specific command, the *Aurora* stream is continuously sampled by an *SPI* interface on the rising edge of the sampling clock. The *SPI* interface buffers the received bytes in its internal *FIFO* until a *DMA* peripheral, configured in double-buffer circular mode, transfers the data to a buffer. In double-buffer mode, the programmer provides the *DMA* with two separate buffers. The *DMA* is then configured to switch back and forth between the buffers every time one of them is full. This allows the rest of the code to transfer data over USB from one of the buffers while the other is being filled, preventing any bit drops.

■ 10.4.2 Pulse injection

The pulse injection circuit is fed by a fast timer output. The width of the timer pulse directly influences the width and amplitude of the generated pulse, which is used for testing the frontends. The size of this pulse has been fixed, and the pulses are generated with a period of 50 µs.

10.5 User board

The user board detection is achieved with the four exposed GPIO pins. When a communication command tries to access the user board, the short ID is first obtained. If the short ID equals `0b1111`, the pins are switched into *I²C* mode, and the microcontroller checks if a configuration header is present in the *EEPROM*.

The following structure of a configuration header has been implemented:

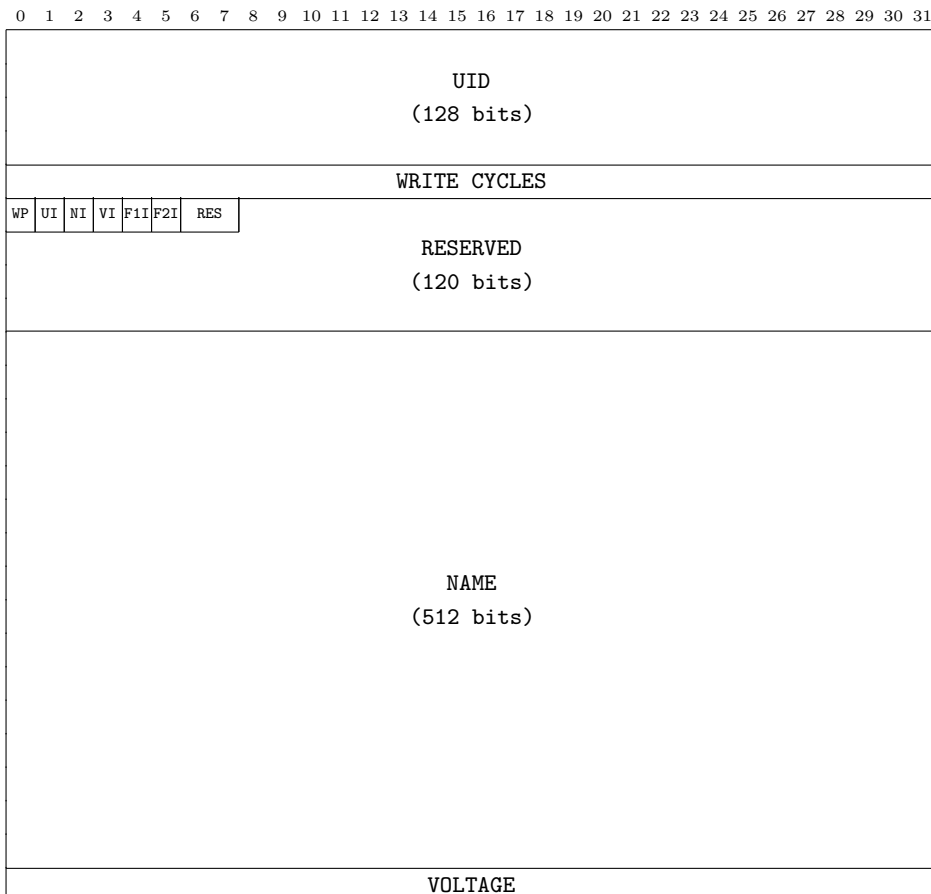


Figure 10.2: EEPROM configuration header structure

where UID is a unique ID generated on the first initialization of the user board, WRITE CYCLES stores the number of times the *EEPROM* has been written. WP is a write-protect bit, and UI, NI, VI, F1I, F2I signal if the UID, name, voltage value, FastIC+ 1, and FastIC+ 2 registers have been initialized, respectively. NAME contains up to a 64-character user name, and VOLTAGE is a floating-point value that stores the high-voltage preset of a given user board.

Chapter 11

Software

A simple Python-based software application was developed to handle basic user tasks. Python was chosen for its simplicity, ease of use, and widespread adoption within the scientific community. However, this choice comes with certain drawbacks, such as reduced performance, which becomes noticeable when processing large amounts of data, such as binary streams from the FastIC+. To address this, efforts were made to optimize the code for speed wherever possible.

11.1 Device communication

The first component of the software is a library of functions for communicating with the device via vendor control transfers and for reading FastIC+ data streams into binary files. The ‘pyusb’ library was utilized for both vendor control transfers and bulk data transfers.

11.2 Stream processing

The second component is a library designed to process the captured data. This library handles synchronization, decoding, and parsing of the data, ultimately outputting FastIC+ packets as objects. It aligns the bitstream using detected Aurora synchronization preambles, reads the block data, descrambles it, and assembles it into packets.

11.3 Example scripts

Finally, these two components were integrated into a simple example script. This script configures the FastIC+ parameters, sets up the HV bias, captures a sample data stream, and decodes it and exports the decoded packets to the user. Additional functionality, such as the comparator calibration procedure, remains to be implemented. These tasks are left either to the users or to the FastIC+ researchers, who, with their in-depth knowledge of the chip, can provide the most efficient implementations.

Chapter 12

Function verification

To verify the functionality of the device, a serie of basic measurements was performed. Later on a more complex test - injecting synthetised pulses to the fastic - was performed and the functionality of the whole device was thus verified.

12.1 Measurements

Multiple measurements were done to verify the basic functionality of the device. A 200 MHz DSO-X 2024A oscilloscope with a 350 MHz probe has been used to carry out the measurements. Measurements on the power supplies were done as close to the supply output as possible. A spring contact was used to contact the ground of the probe to minimize the loop inductance of the probe.

12.1.1 Power supplies

The output ripple of the step down DC/DC converter was measured to be 26 mV peak-to-peak. The frequency of the ripple measured corresponds well to the switching frequency of the converter (750 kHz) which can be seen in Figure 12.1. Note that the cursor frequency is measured over the span of 5 periods to get better accuracy, thus the measured value has to be multiplied by 5. For the LDOs, there was no observable ripple on the output. Both of these confirm that the power network integrity of the device is very good.

12. Function verification

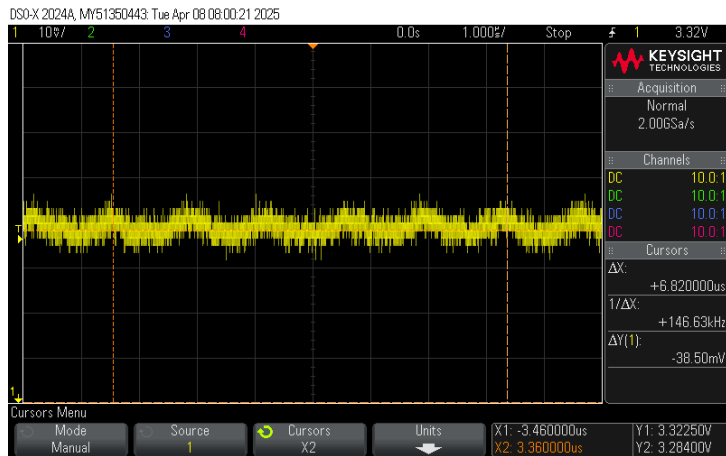


Figure 12.1: Output ripple of the DC/DC converter

12.1.2 High Voltage power supply

Next, the output voltage ripple of the high voltage power supply was measured at 20 V with a $100\text{ k}\Omega$ load connected. The transient response to this load was also measured.

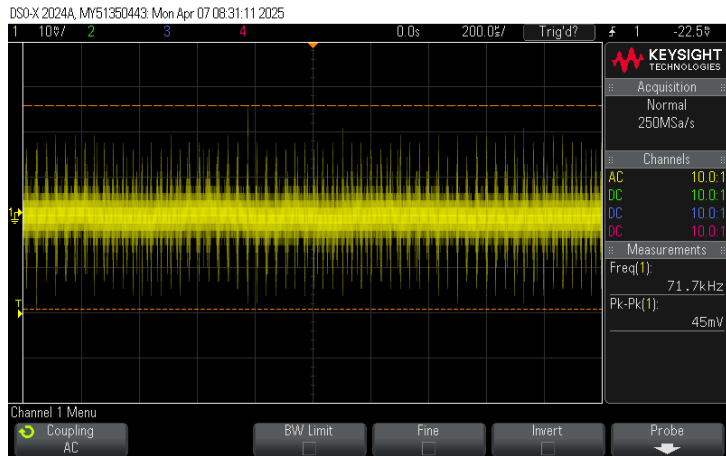


Figure 12.2: Output ripple of the high-voltage power supply



Figure 12.3: Transient response of the high-voltage power supply

From Figure 12.2, it can be seen that a ripple of 45 mV peak-to-peak was observed, which is low enough to avoid causing any issues with the biased sensors. These sensors will experience an even cleaner supply voltage due to the low-pass filtering. Figure 12.3 shows the transient response of the power supply. When the load is connected, the output voltage drops by 100 mV and takes 150 μ s to stabilize back to the setpoint. This will not cause any problems, as this voltage drop is small enough to avoid triggering any other sensors. The typical pulse from the connected sensor will also be much shorter, on the order of a few hundred nanoseconds, causing a much smaller voltage drop. Thus, the evaluated case represents a worst-case scenario.

12.1.3 Pulse injection

The function of the pulse injection circuitry was also verified by measurement, which can be seen in Figure 12.4. The peak voltage of 3.16 V corresponds to a current of approximately 10 mA through the front end. The width of the pulse was set to 200 ns.

**Figure 12.4:** Injected pulse

12.2 Injection pulse test

For the injection pulse test, the FastIC+ 1 was configured to enable the injection signal routing into channel 0. The injection pulse generator was then enabled to generate the injection signal (100 ns pulses with 100 μ s period). Streaming of the aurora data to the USB was then started and 100 ms capture of the bitsream was created. The python library was then used to parse the raw data into packets. The packets for a first packet detection is presented bellow.

```
--- Packet 1 ---
Channel: 0
Packet Type: PKT_TOTLN
Timestamp absolute: 107474.438 us
Pulse Width: 106.249 ns

--- Packet 2 ---
Channel: 8
Packet Type: PKT_TOA_TOTNL
Timestamp absolute: 107474.251 us
Pulse Width: 1032.812 ns

--- Packet 3 ---
Channel: 0
Packet Type: PKT_TOA
Timestamp absolute: 107474.247 us
Pulse Width: 124.218 ns
```

Along with a second detection that is subsequent to the first one.

```
--- Packet 1 ---
Channel: 0
Packet Type: PKT_TOTLN
Timestamp absolute: 107572.038 us
Pulse Width: 107.031 ns

--- Packet 2 ---
Channel: 8
Packet Type: PKT_TOA_TOTNL
Timestamp absolute: 107571.850 us
Pulse Width: 1035.546 ns

--- Packet 3 ---
Channel: 0
Packet Type: PKT_TOA
Timestamp absolute: 107571.846 us
Pulse Width: 125.000 ns
```

The two packets received on channel 0 correspond to the *ToA* of the pulse, transferred in the *PKT_TOA* packet, and the *ToT* transferred in the *PKT_TOTLN*. The third packet on channel 8 is the *ToA* of the trigger pulse generated to start the FSM. These differ due to different thresholds and processing on the separate paths. Taking the relevant information from the first set, it can be seen that a packet with a *ToT* of 106.249 ns was detected at time 107474.247 μ s. The *ToT* corresponds nicely to the generator pulse width. Taking the difference between the *ToA* timestamps of the subsequent detections, the period of the pulses can be calculated as $T = 107571.846 \mu\text{s} - 107474.247 \mu\text{s} = 97.599 \mu\text{s}$, which corresponds to the set period of 100 μs of the injection generator. The inaccuracy of both the *ToA* and *ToT* originates from the injection generator rather than the FastIC+, which is very precise. The purpose of the injection is to easily check that the FastIC+ can receive pulses and process them correctly, rather than verifying the FastIC+'s accuracy.

■ 12.2.1 SiPM S PTR measurement

To verify the device's functionality in a real-world application and stress test the FastIC+ accuracy, a Single Photon Time Resolution (S PTR) measurement with a real SiPM was performed at CERN. In this test, a laser source sends short pulses of light to a *SiPM* sensor connected to the readout. A trigger signal output from the laser is fed into the readout trigger input. On every laser shot, the readout is triggered by the laser and thus generates a *ToA* packet on channel 8. After the beam of light travels to the *SiPM*, it is converted into an electrical pulse and sensed by the FastIC+, which generates the *ToA* and *ToT* packets for the detection. The delay between the trigger *ToA* and the detection *ToA* corresponds to the time the *SiPM* needs to detect

12. Function verification

the photon and generate the electrical pulse, thus the *SPTR* of the *SiPM*.
The *ToT* is used to detect only single-photon events.

**TADY BUDE DALSI KOMENTAR K TOMU EXPERIMENTU
AZ HO CERN UDELA :D**

Chapter 13

Conclusion

In conclusion, the FastIC+ chip was first presented along with its functionality. The communication protocol was described in detail to better explain the reasoning behind the hardware design.

A readout system concept was proposed and the miniature readout system that integrates the FastIC+ along with supporting analog and digital components was developed. A corresponding mechanical enclosure was also designed and fabricated, providing physical protection for field measurements.

Custom firmware was written to enable full functionality of the system, including configuration of the FastIC+ registers, real-time data acquisition, and communication with external control software. To provide an accessible and user-friendly interface, a Python-based software was developed to communicate with the readout from host computer.

The complete readout systems performance was then verified with electrical measurements. A basic pulse injection test was conducted to evaluate the whole reception chain. Finally, the system was deployed in a real-world single-photon time resolution (S PTR) experiment using a silicon photomultiplier (SiPM) at CERN. The device successfully acquired the data which was interpreted and the results presented.

This work represents a comprehensive development effort, from concept to deployment, of a miniature, standalone and versatile readout system based on the FastIC+ chip, suitable for various applications in fast timing and high-energy physics.

Bibliography

- [1] *Aurora 64B/66B Protocol Specification.* https://docs.xilinx.com/v/u/en-US/aurora_64b66b_protocol_spec_sp011. 2014.

List of abbreviations

Abbreviation	Explanation
CERN	Conseil Européen pour la Recherche Nucléaire
ASIC	Application Specific Integrated Circuit
PET	Positron Emission Tomography
TDC	Time-to-Digital Converter
SiPM	Silicon Photo Multiplier
PMT	Photo Multiplier Tube
MCP	Micro Channel Plate
ToA	Time of Arrival
ToT	Time over Threshold
ToF PET	Time of Flight Positron Emission Tomography
LIDAR	Light Detection and Ranging
I2C	Inter-Integrated Circuit
FSM	Finite State Machine
FERO	Front-End Readout
BERO	Back-End Readout
FIFO	First In First Out
MUX	Multiplexer
SLVS	Scalable Low Voltage Signaling
MSB	Most Significant Bit
LSB	Least Significant Bit
BTF	Block Type Field
USB	Universal Serial Bus
FPGA	Field Programmable Gate Array
HDL	Hardware Description Language
IP cores	Intellectual Property Cores
ADC	Analog to Digital Converter
DAC	Digital to Analog Converter
SPI	Serial Peripheral Interface
DMA	Direct Memory Access

Abbreviation	Explanation
TFBGA	Thin Fine Ball Grid Array
MCU	Microcontroller Unit
PLL	Phase Locked Loop
LVDS	Low Voltage Differential Signaling
CMOS	Complementary Metal-Oxide-Semiconductor
EMI	Electromagnetic Interference
SMA	SubMiniature version A
ESD	Electrostatic Discharge
PHY	Physical Layer
ULPI	UTMI+ Low Pin Interface
UTMI	USB Transceiver Macrocell Interface
UCPD	USB Type-C Power Delivery
RMS	Root Mean Square
LD0	Low Dropout Regulator
EEPROM	Electrically Erasable Programmable Read-Only Memory
THT	Through-Hole Technology
PCB	Printed Circuit Board